

## Real-Time Changes in the Optical Spectrum of Organic Semiconducting Films and Their Thickness Regimes during Growth

U. Heinemeyer,<sup>1</sup> K. Broch,<sup>1</sup> A. Hinderhofer,<sup>1</sup> M. Kytka,<sup>1,2</sup> R. Scholz,<sup>3</sup> A. Gerlach,<sup>1</sup> and F. Schreiber<sup>1</sup>

<sup>1</sup>*Institut für Angewandte Physik, Uni Tübingen, 72076 Tübingen, Germany*

<sup>2</sup>*Slovak University of Technology, 812 19 Bratislava, Slovakia*

<sup>3</sup>*Walter Schottky Institut, TU München, 85748 Garching, Germany*

(Received 18 September 2009; published 24 June 2010)

We present real-time *in situ* studies of optical spectra during thin film growth of several prototype organic semiconductors (pentacene, perfluoropentacene, and diindenoperylene) on SiO<sub>2</sub>. These data provide insight into surface and interface effects that are of fundamental importance and of relevance for applications in organic electronics. With respect to the bulk, the different molecular environment and structural changes within the first few monolayers can give rise to significant optical changes. Similar to interface-driven phenomena in, e.g., magnetism, spectral changes as a function of thickness  $d$  are a very general effect, decaying as  $1/d$  in the simplest approximation. We observe energy shifts of 50–100 meV, rather small changes of the exciton-phonon coupling, and new transitions in specific systems, which should be considered as general features of the growth of organics.

DOI: 10.1103/PhysRevLett.104.257401

PACS numbers: 78.66.Qn, 78.20.-e, 78.68.+m

Organic semiconducting thin films have received a tremendous amount of attention due to their potential for device applications, while at the same time many fundamental issues regarding the molecular mechanisms and photophysics of these systems are still open [1]. One of the ubiquitous issues is interface effects, which are of fundamental importance, but for organics they are much less understood than for inorganic systems. Generally, the presence of an interface with its symmetry break and difference in molecular environment will change the structural as well as the optical properties [2], which are, of course, coupled, also affecting the electronic and transport properties [3].

The profound influence of the geometry on the optical properties is already obvious for an isolated molecule described by its Huang-Rhys parameter  $S$  (exciton-phonon coupling). It is responsible for the shape of the vibronic progression observed in absorption [3,4]. In the condensed phase, the coupling to the molecular environment and to possible interfaces enters; see Figs. 1(a1) and 1(a2). The resulting optical spectra arise from a combination of molecular deformations, vibrational degrees of freedom, and intermolecular coupling. All these parameters can change during film growth, where islands nucleate and grow, forming structures potentially different from the bulk, including transient ones. These structural changes have been observed recently [5–7]. Here we focus on the optical properties, namely, absorption. Similar to interface contributions in other areas, e.g., magnetic anisotropies, which dramatically change the behavior, the presence of an interface (associated with a contribution  $\sigma_{\text{int}} \propto 1/\text{area}$ ) can give rise to a thickness dependence ( $d$ ) of the optical properties during growth. The relative weight of volume terms (associated with a contribution  $\rho_{\text{bulk}} \propto 1/\text{volume} \propto$

$1/[d \times \text{area}]$ ) increases with increasing film thickness. In the simplest scenario, where one surface or interface layer differs optically from the bulk [see Figs. 1(b1) and 1(b2)], this results in a  $1/d$  dependence:

$$\rho_{\text{av}} = \rho_{\text{bulk}} + \sigma_{\text{int}}/d. \quad (1)$$

The nature of the thickness dependence is expected to be influenced by the interplay of various coupling parameters [see Figs. 1(a1) and 1(a2)]. Remarkably little is known about these issues for organic semiconducting thin films.

This Letter addresses the fundamental question of how the optical spectra changes with thickness. Surface and interface effects can give rise to, e.g., a shift of the overall energetic position (similar to the solvent shift), a redistribution of oscillator strength (different Huang-Rhys factor  $S$ ), and the appearance or disappearance of a transition. We follow these spectral changes *in situ* and in real time during growth. Selected individual examples in specific regimes have already been studied [8–10]. Most of the pioneering

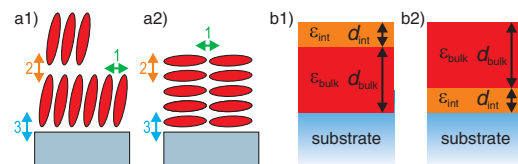


FIG. 1 (color online). (a) Different types of coupling: 1 within one layer, 2 between different layers, 3 with the substrate; (a1) for standing, (a2) for lying molecules. (b) Layer model to account for an optically different (b1) surface and (b2) interface layer of the film. Note that the resulting  $1/d$  dependence of the optical spectra does not discriminate between surface and interface layer. In the text, we refer to both scenarios by using the term interface.

work [9,11] focused on 3,4,9,10-perylene tetracarboxylic dianhydride (PTCDA) thin films, which is a unique and important case, but conceptually different from other systems. While PTCDA forms structures with lying down molecules according to Fig. 1(a2), we present a comprehensive study of a series of other prototypical semiconductors, namely, pentacene (PEN), perfluoropentacene (PFP), and diindenoperylene (DIP) crystallizing with a film morphology according to Fig. 1(a1).

The thin films were grown by organic molecular beam deposition at a base pressure of  $2 \times 10^{-10}$  mbar on Si(100) covered with native oxide ( $\text{Si}_{\text{native}}$ ) and on quartz glass with the back surface roughened to avoid back reflections during the optical measurements. PEN and PFP films were grown at room temperature, whereas DIP films were deposited either at  $T = 130^\circ\text{C}$  [DIP(HT)] or at  $T = -100^\circ\text{C}$  [DIP(LT)] to obtain different degrees of crystalline order.

The film thickness was monitored during growth by a quartz crystal microbalance, which was calibrated by x-ray reflectometry (GE/Seifert, Cu- $K_{\alpha 1}$  radiation, multilayer mirror and double bounce compressor monochromator). For glass substrates the film thickness is determined on a simultaneously grown  $\text{Si}_{\text{native}}$  substrate.

The optical properties of the thin films were studied in real time during film growth by differential reflectance spectroscopy (DRS), which compares the reflectance of an adsorbate-covered [ $R(d)$ ] and a bare substrate ( $R_0$ ):  $\text{DRS} = \frac{R(d)-R_0}{R_0}$  [11]. The DRS data were acquired with a DH-2000 deuterium tungsten halogen light source and a USB2000 spectrometer (Ocean Optics) in the energy range of 1.43–3 eV ( $\Delta\lambda \sim 0.3\text{--}0.4$  nm), measured at normal incidence and averaging over several thousands of spectra to reduce the noise. For data analysis, our own program code based on the matrix formalism for stratified media [12] was employed using a Gaussian oscillator model to describe the dielectric function of the film. The influence of roughness effects was tested in the effective medium approximation and found to result in only minor quantitative changes which do not affect our conclusions [13]. Furthermore, real-time spectroscopic ellipsometry (Woollam M-2000) was also employed. The results are consistent with the DRS data. A detailed discussion of postgrowth spectra can be found in Refs. [14,15]. Here we focus on spectral changes during growth in real time.

We first investigate the overall energy shift during growth, which can be observed for many samples (see Table I). The thickness dependent position of the lowest vibronic subband of the highest occupied molecular orbital (HOMO)–lowest unoccupied molecular orbital (LUMO) transition is plotted in Fig. 2 for PEN on  $\text{Si}_{\text{native}}$  at room temperature. The inset shows the normalized imaginary part of the dielectric function in the energy range of interest. Above a thickness of 2 nm a redshift is clearly visible.

TABLE I. Overview of energy shifts for different samples observed in specific thickness ranges  $\Delta d$ .  $E_{\text{bulk}}$  and  $\Delta E = E_{\text{int}} - E_{\text{bulk}}$  are obtained for PEN films on  $\text{Si}_{\text{native}}$  from a fit based on Eq. (2). For PFP on  $\text{Si}_{\text{native}}$  and for DIP(LT) and DIP(HT) on glass,  $\Delta E$  is estimated from the overall energy shift. Data for PTCDA on mica from Ref. [11].

Sample	$\Delta d$ (nm)	$E_{\text{bulk}}$ (eV)	$\Delta E$ (meV)
PEN ( $\text{C}_{22}\text{H}_{14}$ )	2–20	1.83	$55 \pm 3$
PFP ( $\text{C}_{22}\text{F}_{14}$ )	0.5–20	1.75	$65 \pm 5$
DIP(LT) ( $\text{C}_{32}\text{H}_{16}$ )	0.5–20	2.15	$110 \pm 10$
DIP(HT) ( $\text{C}_{32}\text{H}_{16}$ )	0.5–20	2.25	$0 \pm 0.5$
PTCDA ( $\text{C}_{24}\text{H}_8\text{O}_6$ )	0.3–7	2.23	160

Similar to the solvent shift, the spectra of molecules in the bulk are redshifted compared to those in the outermost layer due to the increased number of nearest neighbors. In the simplest case, i.e., layer by layer growth, the interface contribution together with the bulk contribution results in a  $1/d$  dependence for  $d > d_{\text{int}}$ ; see Eq. (1). In terms of absolute energy positions  $E$  this gives

$$E = E_{\text{bulk}} + \Delta E d_{\text{int}}/d. \quad (2)$$

If the thickness of the interface layer  $d_{\text{int}} = n d_{\text{ML}}$  [16] can be determined, where  $n$  denotes the number of monolayers (MLs), the energy difference  $\Delta E = E_{\text{int}} - E_{\text{bulk}}$  between interface and bulk molecules can be obtained. In the case of PEN on  $\text{Si}_{\text{native}}$ , the fit based on Eq. (2) describes the data above  $d = 2$  nm very well, whereas no energy shift is visible for  $d < 2$  nm; see Fig. 2. According to Ref. [17] PEN grows in the Stranski-Krastanov mode and  $d_{\text{int}} \approx 2$  nm corresponds roughly to 1 ML, or  $n = 1$ . Thus,  $\Delta E = 55$  meV can be determined. In contrast, for PTCDA  $n = 2$  and  $\Delta E = 160$  meV was observed [11,16]. Importantly, for PTCDA the coupling between consecutive layers is

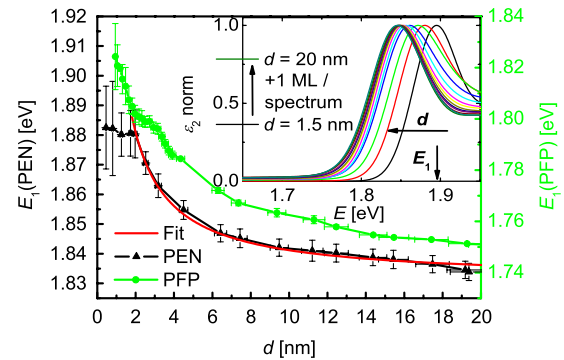


FIG. 2 (color online). Energy position of the first peak for PEN (black curve) and PFP (green curve) on  $\text{Si}_{\text{native}}$  versus film thickness. A fit (red) based on  $E_1 = A + B/d$  with  $A = 1.83$  eV and  $B = 0.099$  eV/nm describes the PEN data for  $d > 2$  nm very well. For  $d < 2$  nm no energy shift is visible for PEN in contrast to PFP. The inset shows the normalized imaginary part of the dielectric function  $\epsilon_2$  of PEN. A redshift with increasing thickness of the HOMO-LUMO transition is clearly visible.

expected to be strong, so that a single ML behaves essentially like a monomer, whereas a bilayer involves the strongest intermolecular interaction along the stacking direction; see Fig. 1(a2). The opposite applies to PEN, PFP, and DIP(HT), which grow standing up on  $\text{Si}_{\text{native}}$  [1,14,18] as visualized in Fig. 1(a1), so that the strongest  $\pi$ - $\pi$  interactions occur within each layer, and monomer behavior is not observed. Therefore, it can be rationalized that the energy shift is smaller than for PTCDA, although it remains surprisingly large.

A redshift is also observed for PFP thin films (on  $\text{Si}_{\text{native}}$ ) ( $\Delta E \approx 65$  meV, see Fig. 2). The similar  $\Delta E$  indicates a comparable interlayer coupling for PEN and for PFP, which is by no means obvious since a similar thin film structure competes with a quite different molecular charge distribution. The exact shape of the curve also suggests subtle, probably morphological differences to PEN, in particular, in the first MLs.

The spectrum of DIP(LT) on glass shifts even more during film growth ( $\Delta E \approx 110$  meV between  $d \approx 0.2$  nm and  $d \approx 15$  nm). It seems to follow a similar mechanism as in PTCDA since at LT the DIP molecules adsorb partly in the lying down configuration, forming a film structure with reduced ordering. Since layer by layer growth does not take place, the interface thickness cannot easily be determined. In contrast, at HT no energy shift but rather an energy splitting is visible for DIP on glass, where the well-ordered  $\sigma$  phase with nearly standing upright molecules forms. Thus, coupling 2 in Fig. 1(a1) is reduced due to the smaller  $\pi$  overlap between the consecutive MLs.

Next we examine the exciton-phonon coupling [3,4]. It can be determined from the vibronic progression in the optical absorption spectra of dissolved molecules or amorphous films. In crystalline films composed of PEN, PFP, and DIP, intermolecular interactions result in modified intensities of consecutive subbands, which therefore cannot be interpreted exclusively in terms of  $S$ , requiring instead an in-depth analysis of intermolecular exciton transfer [19]. PEN and PFP with their transition dipoles along the short axes of the two basis molecules form two Davydov components dominated by neutral molecular excitations, determining in turn different diagonal components of the dielectric tensor [20]. In DIP, the transition dipoles along the long axes of both basis molecules are close to parallel, so that only a single component of the dielectric tensor can be assigned to intramolecular excitations [15].

Obviously the molecular environment affects the intermolecular exciton transfer significantly. A logical consequence of the changing molecular environment (and thus symmetry) during growth would be different selection rules, i.e., the appearance or disappearance of modes. This is of course less a gradual shift than a qualitatively new behavior. New transitions can indeed be found as shown in Fig. 3 for DIP(HT) at 2.8 eV, whereas for PEN

and PFP films there is no evidence for a significant contribution of a new mode appearing below 3 eV.

The vibronic progression of the lowest energy  $\pi - \pi^*$  transition of DIP(HT) [4,15] is clearly visible for all thicknesses ranging from 0.2 to 22 nm. Importantly, there are no spectral changes upon molecular deposition in the sub-ML range observable, whereas the transition around  $E \approx 2.8$  eV increases substantially above 1.6 nm. From the different energy spacing, the different anisotropy (its transition dipole is strongest within the substrate plane in contrast to the other transitions [15]), and the different intensity behavior compared to the first three modes, we conclude that it is not part of the vibronic progression. In order to examine the thickness dependence, the intensity ratio between the new mode and the first mode is plotted in Fig. 4, showing a monotonic increase with thickness. For modeling the thickness dependence, the DIP film is decomposed into two different layers with thicknesses  $d_{\text{int}}$ ,  $d_{\text{bulk}}$  and complex dielectric functions  $\epsilon_{\text{int}}$ ,  $\epsilon_{\text{bulk}}$  [see Figs. 1(b1) and 1(b2)] in analogy to Eq. (1), resulting in an average of

$$\epsilon_{\text{av}} = \begin{cases} \epsilon_{\text{int}} & d < d_{\text{int}} \\ \epsilon_{\text{bulk}} + \frac{d_{\text{int}}}{d}(\epsilon_{\text{int}} - \epsilon_{\text{bulk}}) & d > d_{\text{int}}, \end{cases} \quad (3)$$

with  $d = d_{\text{int}} + d_{\text{bulk}}$  being the total film thickness. Using  $\epsilon_{\text{int}} = \epsilon_{\text{exp}}(d = 1 \text{ nm})$  and  $\epsilon_{\text{bulk}} = \epsilon_{\text{exp}}(d = 22 \text{ nm})$ , this model describes the data well above 3.1 nm, where a  $1/d$  thickness dependence can indeed be observed. This shows that the DIP film involves an interfacial layer which deviates spectrally from the bulklike properties. The inset of Fig. 4 shows data plotted versus  $1/d$  in the spirit of Eq. (3), where the low thickness range is more pronounced, showing that above  $1 \text{ nm}^{-1}$  no significant spectral changes occur. In an intermediate thickness range between 1.5 and 3 nm, the actual behavior is more complex.

This new subband cannot be assigned to the strong intramolecular HOMO-LUMO transition dipoles which produce the dominating component of the dielectric tensor

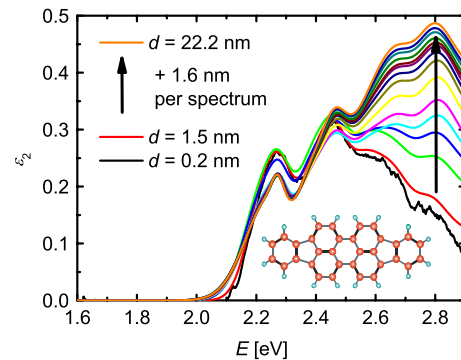


FIG. 3 (color online).  $\epsilon_2(E)$  for a DIP(HT) film grown on glass. The thickness varies in steps of 1.6 nm from 0.2 to 22.2 nm. The modes at 2.25 eV (0-0), 2.48 eV (0-1), and 2.6 eV (0-2) are part of the vibronic progression, whereas the mode at 2.8 eV does not belong to it.

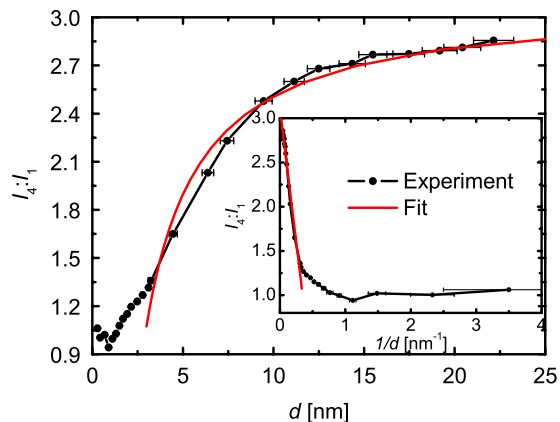


FIG. 4 (color online). Intensity ratio between the new mode ( $I_4$ ) and the lowest transition ( $I_1$ ) of DIP(HT) versus film thickness. The fit is based on Eq. (3).

with a large projection onto the substrate normal and a smaller projection into the substrate plane. Therefore, it is assigned to contributions from Frenkel and charge transfer excitations of higher transitions [15]. It is thus clear that this new mode is a signature of the intermolecular coupling, which is specific for DIP(HT) films, since it does not occur in the monomer spectrum. Furthermore, it is significantly less pronounced for DIP(LT) films, which exhibit less structural order than HT films as proven by x-ray data [13]. It is therefore coupled to the structural order, which increases during film growth as the spectral real-time changes show.

In conclusion, the optical real-time observations of organic films during growth reveal how the dielectric function depends on the film thickness even in the sub-ML range. Different molecules were the subject of our investigation, all of them (PEN, PFP, and DIP) forming crystalline structures, where pronounced optical changes could be observed. The most general effect observed is an overall redshift during growth, which can be understood in terms of dielectric screening with increasing number of molecular neighbors similar to the solvent shift. The spectral shift for molecules at the interface relative to the bulk spectrum

can be determined from the thickness dependence. The most dramatic effect, i.e., the appearance of a new mode due to the intermolecular coupling, was demonstrated for DIP(HT). Overall, our results show that interface-driven spectral features arise from thickness dependent relative weights of the different types of coupling visualized in Fig. 1, which in turn are related to the orientation of the molecules and their transition dipoles.

Financial support by the DFG and the DAAD is gratefully acknowledged.

- [1] *Physical and Chemical Aspects of Organic Electronics*, edited by C. Wöll (Wiley-VCH, Berlin, 2009).
- [2] L. D. Sun *et al.*, *Phys. Rev. Lett.* **96**, 016105 (2006).
- [3] N. Ueno and S. Kera, *Prog. Surf. Sci.* **83**, 490 (2008).
- [4] J. B. Birks, *Photophysics of Aromatic Molecules* (Wiley-Interscience, London, 1970).
- [5] S. Kowarik *et al.*, *Phys. Rev. Lett.* **96**, 125504 (2006).
- [6] S. Kowarik *et al.*, *Phys. Chem. Chem. Phys.* **8**, 1834 (2006).
- [7] A. C. Mayer *et al.*, *Phys. Rev. Lett.* **97**, 105503 (2006).
- [8] O. D. Gordan *et al.*, *Appl. Phys. Lett.* **88**, 141913 (2006).
- [9] H. Proehl *et al.*, *Phys. Rev. Lett.* **93**, 097403 (2004).
- [10] F. Warken *et al.*, *Opt. Express* **15**, 11 952 (2007).
- [11] H. Proehl *et al.*, *Phys. Rev. B* **71**, 165207 (2005).
- [12] J. Lekner, *Theory of Reflection of Electromagnetic and Particle Waves* (M. Nijhoff, Dordrecht, 1987).
- [13] See supplementary material at <http://link.aps.org/supplemental/10.1103/PhysRevLett.104.257401> for a more detailed description of the DRS data analysis and the investigation of the influence of roughness. In addition, x-ray data are presented for demonstrating the structural difference between DIP(HT) and DIP(LT) samples.
- [14] A. Hinderhofer *et al.*, *J. Chem. Phys.* **127**, 194705 (2007).
- [15] U. Heinemeyer *et al.*, *Phys. Rev. B* **78**, 085210 (2008).
- [16] V. M. Agranovich *et al.*, *Chem. Phys. Lett.* **199**, 621 (1992).
- [17] S. Kowarik *et al.*, *Thin Solid Films* **515**, 5606 (2007).
- [18] A. C. Dürr *et al.*, *Phys. Rev. Lett.* **90**, 016104 (2003).
- [19] L. Gisslén *et al.*, *Phys. Rev. B* **80**, 115309 (2009).
- [20] M. Dressel *et al.*, *Opt. Express* **16**, 19770 (2008).